Physica C: Superconductivity and its applications 550 (2018) 52–56

Contents lists available at ScienceDirect

Physica C: Superconductivity and its applications

journal homepage: www.elsevier.com/locate/physc

New proposal of mechanical reinforcement structures to annular REBaCuO bulk magnet for compact and cryogen-free NMR spectrometer

H. Fujishiro[a,*], K. Takahashi[a], T. Naito[a], Y. Yanagi[b], Y. Itoh[b], T. Nakamura[c]

[a] Faculty of Science and Engineering, Iwate University, 4-3-5 Ueda, Morioka 020-8551, Japan
[b] IMRA Material R&D Co., Ltd., 2-1 Asahi-machi, Kariya 448-0032, Japan
[c] RIKEN, 2-1 Hirosawa, Wako 351-0198, Japan

ABSTRACT

We have proposed new reinforcement structures using an aluminum alloy ring to the annular REBaCuO bulks applicable to compact and cryogen-free 400 MHz (9.4 T) nuclear magnetic resonance (NMR) spectrometer using a numerical simulation of mechanical stress. The thermal compressive stress, σ_θ^{cool}, which was applied to the annular bulks during cooling due to the difference of thermal expansion coefficient between bulk and aluminum alloy, became fairly enhanced at the surface of the uppermost bulk for the new reinforcement structures, compared to the conventional reinforcement with the same height as the annular bulk, in which the compressive σ_θ^{cool} value was reduced. During field-cooled magnetization (FCM), the electromagnetic hoop stress, σ_θ^{FCM}, became the maximum at the innermost edge of the uppermost ring bulk at intermediate time step. The actual total hoop stress, σ_θ ($= \sigma_\theta^{cool} + \sigma_\theta^{FCM}$), due to both cooling and FCM processes was also analyzed and the new ring structures are fairly effective to reduce the σ_θ value and became lower than the fracture strength of the bulk. The new reinforcement structures have a possibility to avoid the fracture of the bulks and to realize a 400 MHz NMR spectrometer.

1. Introduction

Nuclear magnetic resonance (NMR) spectrometer with high resolution using superconducting coils is a powerful apparatus to analyze complex molecular structure or to develop new drugs. Recently, a compact and cryogen-free NMR spectrometer with a medium resolution of 200 MHz (4.7 T) has been developed using annular REBaCuO superconducting bulks (RE: rare earth element), in which the NMR spectra of ethanol with a full width at half of the maximum (FWHM) of 0.1 ppm (21 Hz) have been achieved [1]. The magnetic resonance imaging (MRI) was also investigated using the same apparatus [2]. In the apparatus, the annular REBaCuO bulks are magnetized by field-cooled magnetization (FCM), in which large hoop and radial stresses are experienced and the bulks are sometimes fractured for higher applied field. The metal ring support must be considered to avoid the bulk fracture. We have investigated numerically and experimentally the mechanical stresses (hoop stress, σ_θ, and radial stress, σ_r) in the finite REBaCuO annular bulk reinforced by metal ring with the same height as that of the bulk during FCM [3,4,5]. The thermal hoop stress, σ_θ^{cool}, was also estimated, which was applied to the bulk when cooling down to operating temperature due to the difference of thermal expansion coefficient between bulk and metal ring. As a result, it was found that the compressive σ_θ^{cool} was reduced fairly at the uppermost surface of the finite bulk because of the larger thermal compression of the metal ring along the axial direction. The total hoop stress during FCM under cooling, σ_θ ($= \sigma_\theta^{cool} + \sigma_\theta^{FCM}$), was larger than the results for the infinite ring bulk reinforced by the metal ring with infinite height [4]. These analytical results are valuable to compare to the mechanical strength of the bulk material and to judge the bulk fracture during FCM.

In this paper, we performed the numerical simulation of the electromagnetic properties (trapped field, B_z, and induced persistent supercurrent density, J_θ) and the hoop stress, σ_θ, in the actual annular REBaCuO bulks reinforced by new mechanical reinforcement structures of aluminum alloy ring during FCM from B_{ex} = 9.4 T at 50 K using the finite element method (FEM) to realize the 400 MHz (9.4 T) NMR spectrometer safely. The effectiveness of the new reinforcement structure of the metal ring is deduced to reduce the total hoop stress.

2. Numerical simulation framework

Based on our experimental setup with eight stacked annular REBaCuO bulks [6], we prepared the following framework of three-

* Corresponding author.
E-mail address: fujishiro@iwate-u.ac.jp (H. Fujishiro).

https://doi.org/10.1016/j.physc.2018.04.012
Received 25 February 2018; Received in revised form 11 April 2018; Accepted 17 April 2018
Available online 23 April 2018
0921-4534/

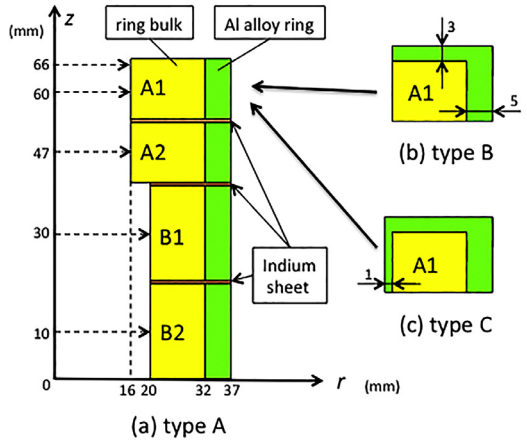

Fig. 1. Schematic models of a conventional reinforcement structure ((a) type A) and two new reinforcement structures ((b) type B and (c) type C).

dimensional (3D) numerical simulation for the FCM procedure. Schematic views of three types of numerical half models are presented in Fig. 1. In Fig. 1(a), two end bulks named "A1" and "A2" (64 mm outer diameter (O.D.), 32 mm inner diameter (I.D.) and 13 mm height (H)) and two inner bulks named "B1" and "B2" (64 mm O.D., 40 mm I.D. and 20 mm H) were vertically stacked along z-direction, all of which were reinforced by the aluminum alloy ring 5 mm in width with the same height as the bulks. Aluminum alloy (A7075) is a suitable material for the reinforcement of the bulk applied to NMR apparatus because of non-magnetic and higher mechanical strength, compared to pure aluminum. Indium thin foils 0.1 mm in thickness were inserted between bulks with rings for better thermal contact. This model is abbreviated as "type A", which is a conventional reinforcement structure [4]. We propose two types of new reinforcement structures. In the "type B" model, the ring plate made by aluminum alloy 3 mm in thickness is integrally molded to the "A1" bulk of the "type A" model shown in Fig. 1(b). In the "type C" model, the inner ring made by aluminum alloy 1 mm in thickness is further molded to the "A1" bulk of the "type B" model, as shown in Fig. 1(c).

The bulk sets were magnetized by FCM using an infinite solenoid coil (150 mm O.D., 100 mm I.D. and infinite H). Physical phenomena in the FCM simulation are described using an electromagnetic equation based on the axisymmetric coordinate system [7,8], in which the temperature of the REBaCuO bulks is assumed to be constant at $T_s = 50$ K during FCM. Because temperature rise is pretty small during FCM in the experiment. The power-n model ($n = 100$) was used to describe the nonlinear E–J characteristic of the bulk. The critical current density, J_c ($= 9.6 \times 10^8$ A/m^2) flowing in the ab-plane of the bulk, which is about twice as large as that at $T_s = 50$ K for the REBaCuO bulk [9], is assumed to be independent of magnetic field to realize the approximate Bean's model [10]. In the simulation process of FCM, a magnetic field of $B_{ex} = 9.4$ T was applied above the critical temperature, T_c ($= 92$ K), and then the bulk was cooled to $T_s = 50$ K. Thereafter, the magnitude of the magnetic field was monotonically decreased from B_{ex} to zero in 10 steps, as shown in the inset of Fig. 2(a).

In an isotropic material, Hooke's law is established, in which the stress is linearly proportional to the strain [4]. Since the REBaCuO bulk consists of c-axis oriented $REBa_2Cu_3O_7$ matrix phase, dispersed by non-superconductive fine particles such as RE_2BaCuO_5 and Ag, the mechanical properties are anisotropic. The mechanical strength of the REBaCuO bulk in the ab-plane is fairly larger than that along the c-axis direction [11,12]. In the present numerical simulation, the REBaCuO bulk is assumed to be isotropic and homogeneous and mechanical parameters (Young's modulus and thermal contraction coefficient) in the ab-plane were used for simplicity. Because the electromagnetic and thermal hoop stresses, σ_θ, are applied in the ab-plane of the bulk. The

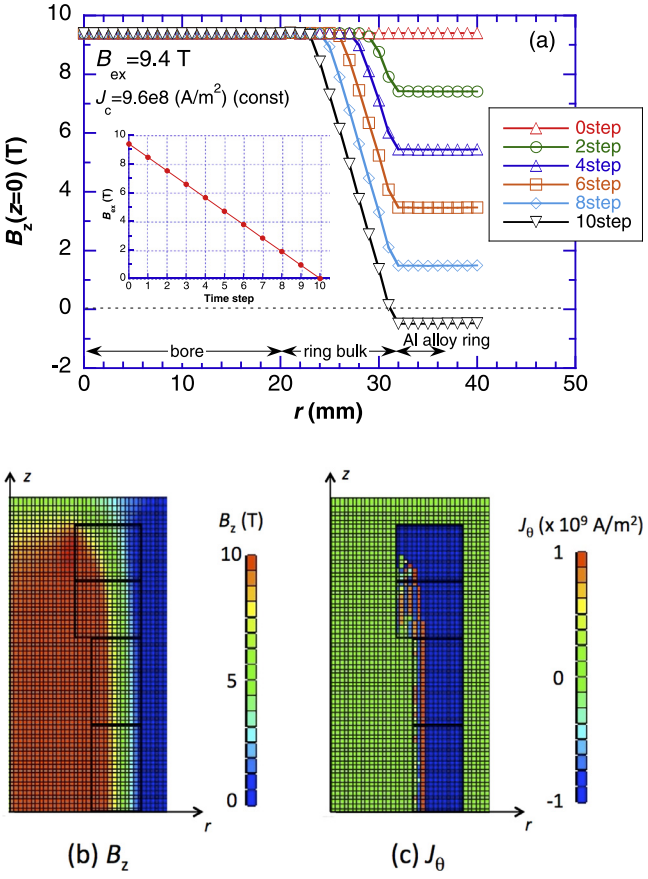

Fig. 2. (a) Time step dependence of the cross-sectional plots of the trapped field, $B_z(r)$, for the annular REBaCuO bulks during FCM from $B_{ex} = 9.4$ T. Contour maps of the (b) trapped field, B_z, and (c) persistent current density, J_θ, at the final (10th) step are shown. (For interpretation of the references to colour in this figure legend, the reader is referred to the web version of this article.)

electromagnetic hoop stress, σ_θ^{FCM}, was estimated for each step of FCM, which acts circumferentially on each end face of the meshed element [13,14]. The thermal hoop stress, σ_θ^{cool}, by cooling from 300 to 50 K was also estimated for each reinforcement structure. The mechanical parameters (Young's modulus, E, Poisson ratio, ν, and thermal expansion coefficient, α) of the REBaCuO bulk, aluminum alloy, and indium sheet used in the elastic simulation are summarized in Table 1. Commercial software, Photo-Eddy and Photo-ELAS (Photon Ltd., Japan) were used for the analyses of the electromagnetic properties and mechanical stresses.

3. Results and discussion

3.1. Trapped field, B_z, and induced current density, j_θ

Fig. 2(a) shows the time step dependence of the cross-sectional plots of the trapped field, $B_z(r)$, at $z = 0$ for the annular REBaCuO bulks during FCM from $B_{ex} = 9.4$ T. The external magnetic field decreased step by step without a field slope due to the infinite length of

Table 1
Mechanical properties (E: Young's modulus, ν: Poisson ratio, α: thermal contraction coefficient) used in the numerical simulation [13].

	E (GPa)	ν	α (K^{-1})
REBaCuO bulk	100	0.33	5.2×10^{-6}
Al alloy ring	78	0.34	1.66×10^{-5}
Indium sheet	110	0.44	3.25×10^{-5}

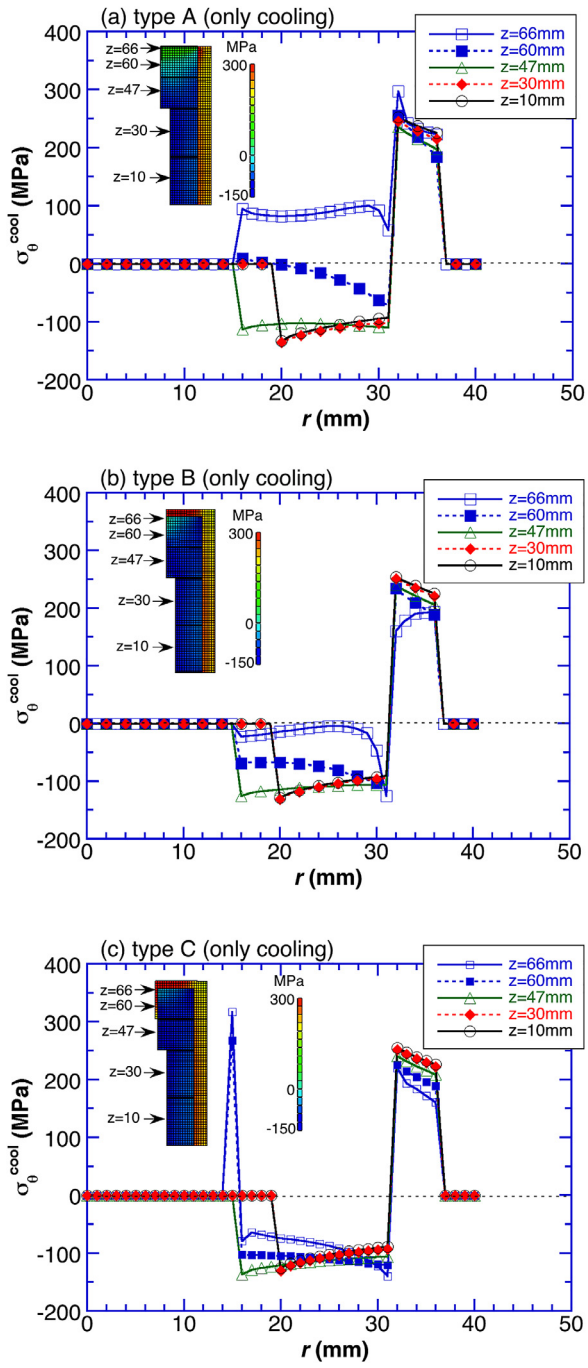

Fig. 3. The radius (r) dependence of the thermal hoop stress, σ_θ^{cool}, for the annular REBaCuO bulks reinforced by three types of aluminum alloy rings for each z-position under cooling from 300 to 50 K. Inset of each figure shows the contour map of the σ_θ^{cool}.

magnetizing solenoid coil. In the annular bulk periphery, the magnetic field monotonically decreases with increasing time step and has a constant field slope, which is equivalent to a constant critical current density, J_c, based on Bean's model. The B_z value at $z = r = 0$ was maintained to 9.4 T up to the final (10th) step due to the large J_c value. Fig. 2(b) and (c), respectively, show the contour maps of the trapped field, B_z, and the persistent current density, J_θ, at the final step. The B_z profile is rounded at the top surface of the "A1" bulk, where the persistent current similar to J_c flows even at the surface of the "A1" bulk, as shown in the blue region in Fig. 2(c).

3.2. Thermal hoop stress, σ_θ^{cool}, under cooling from 300 to 50 K

Fig. 3 shows the radius (r) dependence of the thermal hoop stress, σ_θ^{cool}, in the annular bulks reinforced by three types of aluminum alloy rings at various z-positions under the cooling from 300 to 50 K without FCM. The contour map of the σ_θ^{cool} is shown in the inset of each panel. In Fig. 3(a) for the conventional "type A", a thermally compressive stress ($\sigma_\theta^{cool} < 0$) is effectively applied to the "A2", "B1" and "B2" bulks, and a tensile stress ($\sigma_\theta^{cool} > 0$) is applied to the aluminum alloy ring region ($32 \le r \le 37$ mm), because the thermal expansion coefficient, α, of the aluminum alloy is about three times larger than that of the REBaCuO bulk, as shown in Table 1. However, it is surprising that the α_θ^{cool} value at the top surface of the "A1" bulk ($z = 66$ mm) is positive (tensile stress), which is as large as +100 MPa. Because of the larger α value of the aluminum alloy, the aluminum alloy rings shrink along both z- and r-directions. During cooling, the annular bulks were fastened along the r-direction and, at the same time, were pulled along the z-direction toward $z = 0$, assuming not to slip between bulk and metal ring. As a result, the compressive hoop stress of the "A1" bulk became fairly weak and changed to the large positive value [4].

In Fig. 3(b) for the new "type B" reinforcement, the large positive α_θ^{cool} value of "A1" bulk in "type A" was drastically reduced and changed to weak negative value. This result strongly suggests that the upper plate effectively acts to reduce the expansion of the aluminum alloy ring along the r-direction. In Fig. 3(c) for another new "type C" reinforcement, the reduction of the positive σ_θ^{cool} value becomes more effective by the additional thin ring support in the inner periphery of the "A1" bulk, compared to the "type B" reinforcement. The compressive σ_θ^{cool} value is further enhanced in the "A1" bulk. As a result, the compressive σ_θ^{cool}, which is larger than −70 MPa is applied for all the annular bulks during cooling procedure. Note that the σ_θ^{cool} value of the inner ring support is positive and is as high as +250 MPa, which is, however, smaller than the fracture strength of the aluminum alloy.

3.3. Electromagnetic hoop stress, σ_θ^{FCM} during FCM

During FCM, the electromagnetic hoop stress is applied to the annular bulks. Fig. 4(a) shows the cross-sectional plots of the electromagnetic hoop stress, σ_θ^{FCM}, for the annular bulks with the "type A" reinforcement at the 6th step of FCM, in the case that there is no cooling. The contour map of the σ_θ^{FCM} is shown in the inset. The maximum σ_θ^{FCM} is achieved at the innermost periphery edge of each annular bulk. The σ_θ^{FCM} value gradually decreases with increasing r, but steeply drops at the interface ($r = 32$ mm) between bulk and aluminum alloy ring, which results from the smaller Young's modulus, E, of the aluminum alloy ring. Note that the σ_θ^{FCM} depends on the B_{ex} and J_c values. Fig. 4(b) and (c), respectively, show the same plots of σ_θ^{FCM} for the annular bulks with the "type B" and "type C" reinforcement at the 6th step of FCM. The similar characteristics are observed to that for the "type A", but the magnitude of the σ_θ^{FCM} value decreased and the $\sigma_\theta^{FCM}(r)$ profiles changed depending on the reinforcement structure of the aluminum ring.

Fig. 5 shows time step dependence of the maximum electromagnetic hoop stress, σ_θ^{FCM}(max), in each annular bulk with the three types of reinforcements during FCM from 9.4 T. For each case, σ_θ^{FCM}(max) increases with increasing FCM time step, takes a maximum at the intermediate step, and then decreases with increasing time step for each bulk and each reinforcement. However, the magnitude and the time step dependence of σ_θ^{FCM}(max) change depending on the reinforcement structure. In Fig. 5(a) for the conventional "type A" reinforcement, the σ_θ^{FCM}(max) value is larger, compared to those for the "type B" and "type C" reinforcements. The "type C" reinforcement is the most effective to reduce the electromagnetic hoop stress during FCM.

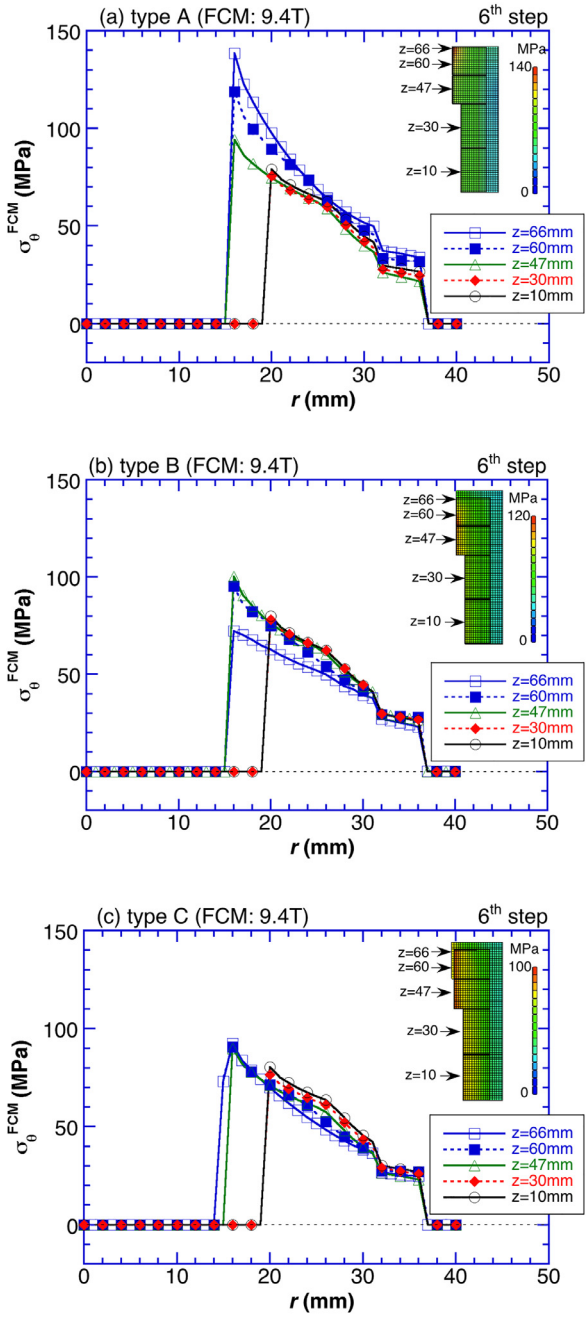

Fig. 4. Cross-sectional plots of the electromagnetic hoop stress, σ_θ^{FCM}, for the annular bulks with the (a) "type A", (b) "type B" and (c) "type C" reinforcements at the 6th step of FCM from B_{ex} = 9.4 T, without cooling.

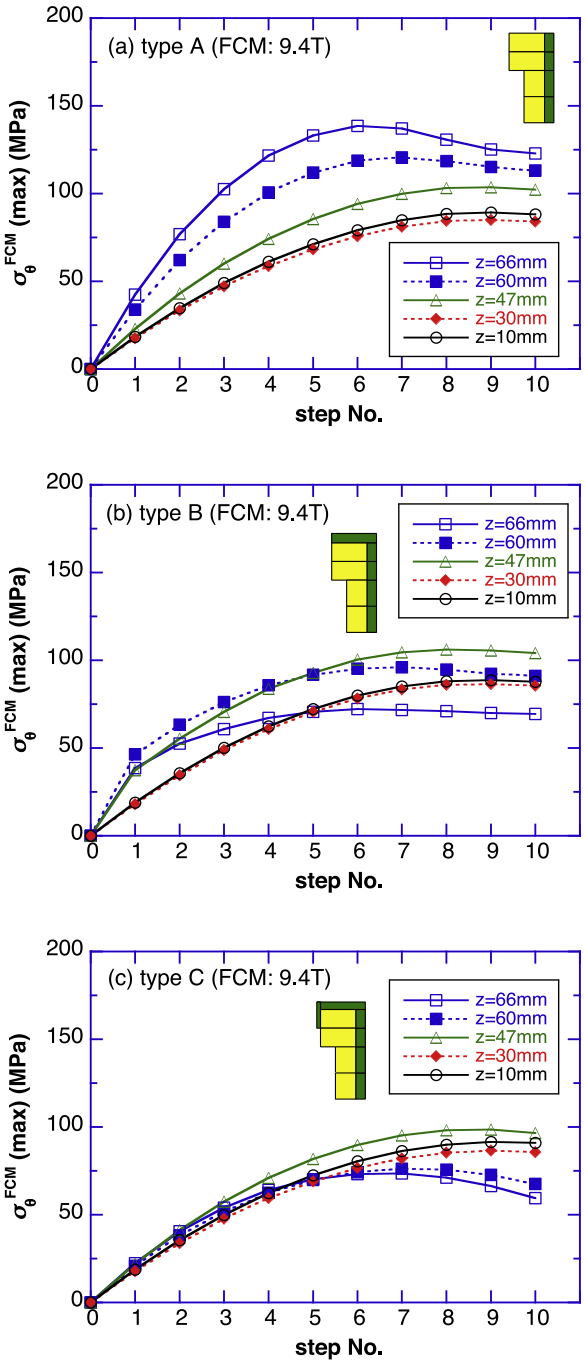

Fig. 5. Time step dependence of the maximum electromagnetic hoop stress, σ_θ^{FCM}(max), in each annular bulk with the three types of aluminum alloy ring reinforcements ((a) conventional "type A", (b) new "type B" and (c) new "type C") during FCM from B_{ex} = 9.4 T.

3.4. Total hoop stress, σ_θ during FCM under cooling

In the actual FCM process, both the thermal and electromagnetic stresses must be considered from both the cooling and the FCM process. Fig. 6 shows the radius (r) dependence of the total hoop stress, σ_θ ($= \sigma_\theta^{cool} + \sigma_\theta^{FCM}$), at the 6th step at various z-positions in the annular bulks reinforced by three types of the reinforcements, under both the cooling process (σ_θ^{cool}) from 300 to 50 K and the FCM process (σ_θ^{FCM}) from 9.4 T. In the Fig. 6(a) for the "type A" reinforcement, the σ_θ value increased positively in the annular bulks by the superposition; σ_θ was +235 MPa at r = 16 mm and z = 66 mm (near the top surface of the "A1" bulk), but the σ_θ was negative for other annular bulks. These results suggest that the "A1" bulk might be broken by the fairly larger electromagnetic hoop stress than the mechanical strength of 30–100 MPa [15,16], during the actual FCM process from 9.4 T. For the "type B" reinforcement shown in Fig. 6(b), the larger tensile σ_θ value was fairly reduced to +116 MPa only at the innermost periphery of the surface of the "A1" bulk. Furthermore, for the "type C" reinforcement shown in Fig. 6(c), the σ_θ value was further reduced to be smaller than +17 MPa even for the "A1" bulk, in which all annular bulks will never break during FCM even from 9.4 T. However, the large positive σ_θ value is applied in the inner ring support of the "type C" reinforcement, which is, however, lower than the fracture strength of the aluminum alloy.

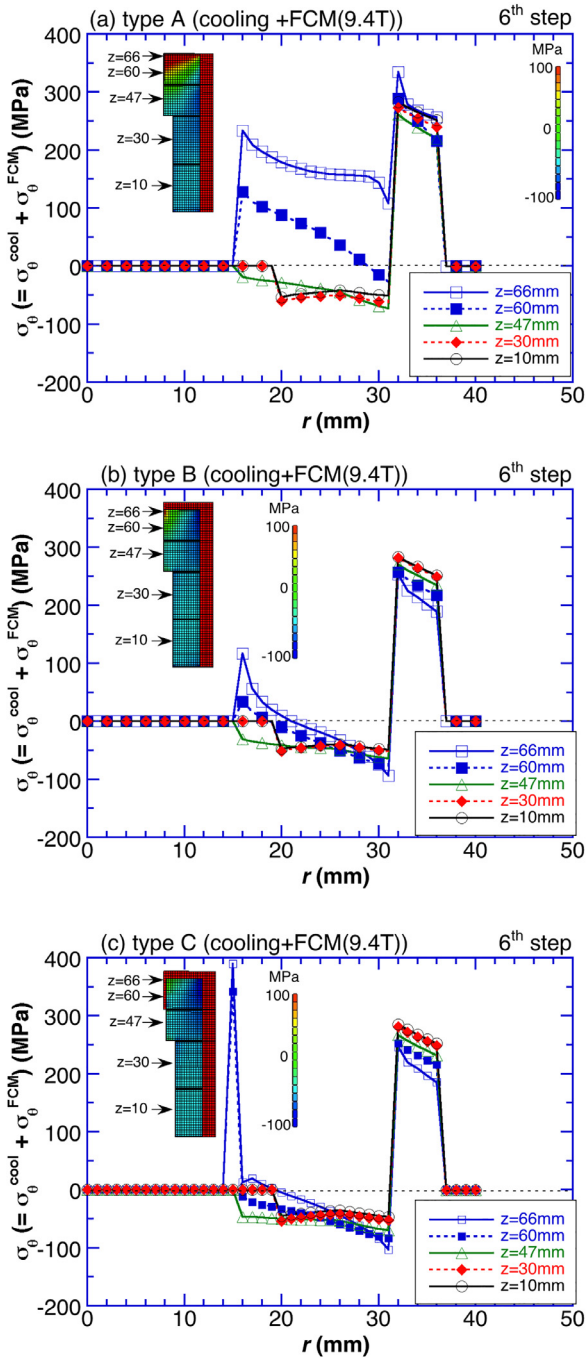

Fig. 6. The radius (r) dependence of the total hoop stress, σ_θ ($= \sigma_\theta^{cool} + \sigma_\theta^{FCM}$), value at the 6th step at various z-positions in the finite ring bulk reinforced by three types of the reinforcements ((a) conventional "type A", (b) new "type B", and (c) new "type C"), under both the cooling process (σ_θ^{cool}) from 300 to 50 K and the FCM process (σ_θ^{FCM}) of B_{ex} = 9.4 T.

4. Conclusion

We have performed numerical simulation of the hoop stress, σ_θ, in the actual annular REBaCuO bulks reinforced by three types of reinforcements using aluminum alloy ring during FCM from B_{ex} = 9.4 T at 50 K. The important analytical results and conclusions are summarized as follows.

(1) The thermal hoop stress, σ_θ^{cool}, which was applied to the annular bulks during cooling, changed depending on the shape of the aluminum alloy reinforcement. For the conventional metal ring reinforcement ("type A"), a large tensile stress was applied at the surface of the end bulk. The new proposed "type B" reinforcement structure with a ring plate to the end bulk of "type A" is effective to reduce the tensile stress. Furthermore, another new "type C" reinforcement structure with an inner ring to the end bulk of "type B" is more effective.
(2) The electromagnetic hoop stress, σ_θ^{FCM}, also changed depending on the shape of the aluminum alloy reinforcement and became the maximum at the innermost edge of the uppermost ring bulk at intermediate step in FCM.
(3) The actual total hoop stress, σ_θ ($= \sigma_\theta^{cool} + \sigma_\theta^{FCM}$), due to both cooling and FCM processes was analyzed for three types of aluminum alloy reinforcements. As a result, the "type C" reinforcement was confirmed to be fairly effective to reduce the total hoop stress and to have a possibility to avoid the mechanical fracture of the annular bulks.

Acknowledgements

This research is partially supported by a "Development of Systems and Technologies for Advanced Measurement and Analysis" from Japan Agency for Medical Research and development, AMED, and from JSPS KAKENHI grant no. 15K04646.

References

[1] T. Nakamura, D. Tamada, Y. Yanagi, Y. Itoh, T. Nemoto, H. Utumi, K. Kose, J. Magn. Reson. 259 (2015) 68–75.
[2] D. Tamada, T. Nakamura, Y. Itoh, K. Kose, Physica C 492 (2013) 174-147.
[3] H. Mochizuki, H. Fujishiro, T. Naito, Y. Itoh, Y. Yanagi, T. Nakamura T, IEEE Trans. Appl. Supercond. 26 (2016) 6800205.
[4] H. Fujishiro, M.D. Ainslie, K. Takahashi, T. Naito, Y. Yanagi, Y. Itoh, T. Nakamura, Supercond. Sci. Technol. 30 (2017) 085008.
[5] K. Takahashi, H. Fujishiro, T. Naito, Y. Yanagi, Y. Itoh, T. Nakamura, Supercond. Sci. Technol. 30 (2017) 115006.
[6] Y. Itoh, Y. Yanagi, T. Nakamura, J. Cryo. Super-cond. Soc. Jpn. 52 (2017) 25–32 (in Japanese).
[7] H. Fujishiro, T. Naito, Supercond. Sci. Technol. 23 (2011) 105021.
[8] H. Fujishiro, H. Mochizuki, M.D. Ainslie, T. Naito, Supercond. Sci. Technol. 29 (2016) 084001.
[9] H. Fujishiro, Y. Itoh, Y. Yanagi, T. Nakamura, Supercond. Sci. Technol. 28 (2015) 095018.
[10] C.P. Bean, Phys. Rev. Lett. 8 (1962) 250–253.
[11] A. Murakami, K. Katagiri, K. Kasaba, K. Noto, H. Teshima, M. Sawamura, N. Sakai, M. Murakami, Physica C 412–414 (2004) 673–677.
[12] K. Katagiri, T. Sato, A. Murakami, K. Kasaba, Y. Shoji, K. Noto, H. Teshima, M. Sawamura, Physica C 426–431 (2005) 709–713.
[13] Y. Ren, R. Weinstein, J. Liu, R.P. Sawh, C. Foster, Physica C 251 (1995) 15–26.
[14] T.H. Johansen, Phys. Rev. B 60 (1999) 9690–9703.
[15] D. Lee, K. Salama, Jpn. J. Appl. Phys. 29 (1990) L2017–L2019.
[16] H. Fujimoto, A. Murakami, Supercond. Sci. Technol. 25 (2012) 054017.